34th Annual International Conference of the IEEE EMBS
San Diego, California USA, 28 August - 1 September, 2012

Myofiber Orientation and Electrical Activation in Human and Sheep Atrial Models

Jichao Zhao[1], Martin W. Krueger[2], Gunnar Seemann[2], Shu Meng[1], Henggui Zhang[3], Olaf Dössel[2], Ian J LeGrice[1,4], Bruce H Smaill[1,4]

Abstract— **Anatomically realistic computational models provide a powerful platform for investigating mechanisms that underlie atrial rhythm disturbances. In recent years, novel techniques have been developed to construct structurally-detailed, image-based models of 3D atrial anatomy. However, computational models still do not contain full descriptions of the atrial intramural myofiber architecture throughout the entire atria. To address this, a semi-automatic rule-based method was developed for generating multi-layer myofiber orientations in the human atria. The rules for fiber generation are based on the careful anatomic studies of Ho, Anderson and co-workers using dissection, macrophotography and visual tracing of fiber tracts. Separately, a series of high color contrast images were obtained from sheep atria with a novel confocal surface microscopy method. Myofiber orientations in the normal sheep atria were estimated by eigen-analyis of the 3D image structure tensor. These data have been incorporated into an anatomical model that provides the quantitative representation of myofiber architecture in the atrial chambers. In this study, we attempted to compare the two myofiber generation approaches. We observed similar myo-bundle structure in the human and sheep atria, for example in Bachmann's bundle, atrial septum, pectinate muscles, superior vena cava and septo-pulmonary bundle. Our computational simulations also confirmed that the preferential propagation pathways of the activation sequence in both atrial models is qualitatively similar, largely due to the domination of the major muscle bundles.**

I. INTRODUCTION

Atrial fibrillation (AF) is the most common heart rhythm disturbance, during which the normal regular electrical impulses generated by the sinoatrial node (SAN) are overwhelmed by disorganized electrical impulses. Regional conduction velocity and direction are determined solely by local myofiber orientation and conductivities, as well as wavefront propagation direction. Electrical activation propagates faster along the long-axis of myofibers than the direction perpendicular to them. Though the crucial role of atrial intramural myofiber architecture in AF has been long realized and studied for the past decade [1], [2], the atria have not been as systematically studied and quantified as have ventricles using histological techniques and diffusion tensor magnetic resonance imaging (DTMRI). The reason is likely due to their complicated structure and extremely thin walls. Anatomically realistic computational models provide a powerful platform for analyzing the mechanisms that underlie atrial re-entrant arrhythmias. This view has motivated the development of numerous atrial electrical models with integration of varying degrees of fiber orientations [3], [4].

Currently there are a number of different approaches to describe atrial myofiber orientations. The first is the careful anatomic studies by Ho and co-workers using dissection, macrophotography and visual tracing of fiber tracts [1]. Our understanding of atrial fiber arrangement and preferential conduction pathways is largely based on their work. However, their work is purely descriptive and can not be directly used in computational models. The second is a rule-based approach. Initially, only specialized conduction tracts such as Bachmann's bundle (BB) or crista terminalis (CT) were quantitatively described [4]. Recently, Krueger and co-workers developed a robust semi-automatic method to generate multi-layer myofiber orientations throughout the human atria (obtained by CT, MRI or photography) and incorporated them into computational model [5], [6]. Lastly, one can employ the structure tensor approach developed in materials science to extract myofiber information based on the color intensity gradients of original images. Using this method, Zhao and his colleagues have been able to develop a sheep atrial model incorporating a full detailed description of atrial myofiber structure [7].

In this paper, we seek to compare the general pattern of myofibers in human atria using a rule-based algorithm and sheep atria based on structure tensor approach and determine their effects on electrical activation in computational models. We will illustrate the crucial role of fiber anisotropy in these models, and discuss the steps that are necessary to extend both approaches for fiber generation.

II. METHODS

A. Rule-based fiber generation for human atria

First, the center surface between atrial epicardial and endocardial surfaces was obtained by solving Poisson′s equation. Then user provides the coordinates of twenty-two carefully selected seed points in the right and left atrium. From the seed points, auxiliary lines and further landmarks are calculated using an adapted 3D fast marching level set method to determine the shortest paths between different coordinates in tissue regions without domination of muscular

Manuscript received March 29, 2012. This work is made possible by funding from Health Research Council and National Heart Foundation of New Zealand, and the European Community Seventh Framework Programme (FP7/2007-2013) under grant agreement no 224495 (euHeart project). Correspondence to: Dr. Jichao Zhao, Auckland Bioengineering Institute, University of Auckland, New Zealand. j.zhao@auckland.ac.nz

[1]Auckland Bioengineering Institute, University of Auckland, New Zealand.

[2]Institute of Biomedical Engineering, Karlsruhe Institute of Technology (KIT), Germany.

[3]School of Physics and Astronomy, University of Manchester, UK.

[4]Department of Physiology, University of Auckland, New Zealand.

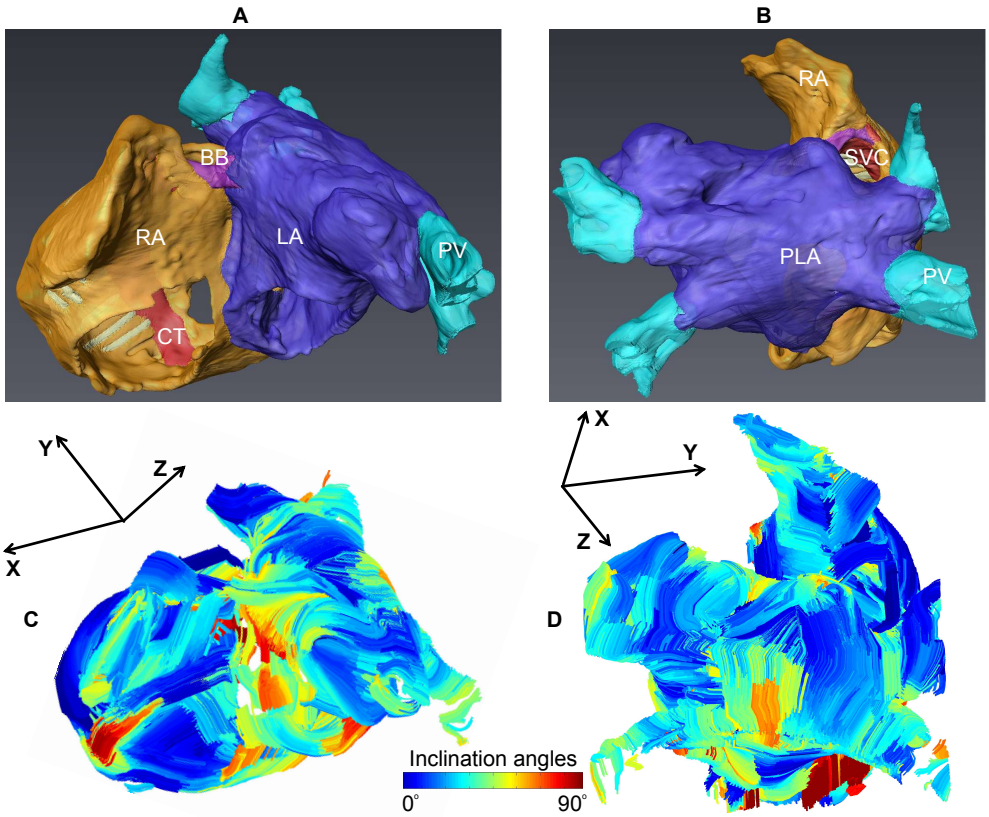

Figure 1: Anatomical structure and intramural myofiber orientation of the human atria. The RA, LA, BB, PVs, PLA, SVC and CT are displayed from an anterior and posterior view in **(A)** and **(B)** respectively. Atrial intramural myofiber orientation was displayed in **(C)** and **(D)**, colour bar represents absolute inclination angle with $\alpha = 0^\circ$ parallel to the X-Y plane and $\alpha = 90^\circ$ corresponding to the Z axis.

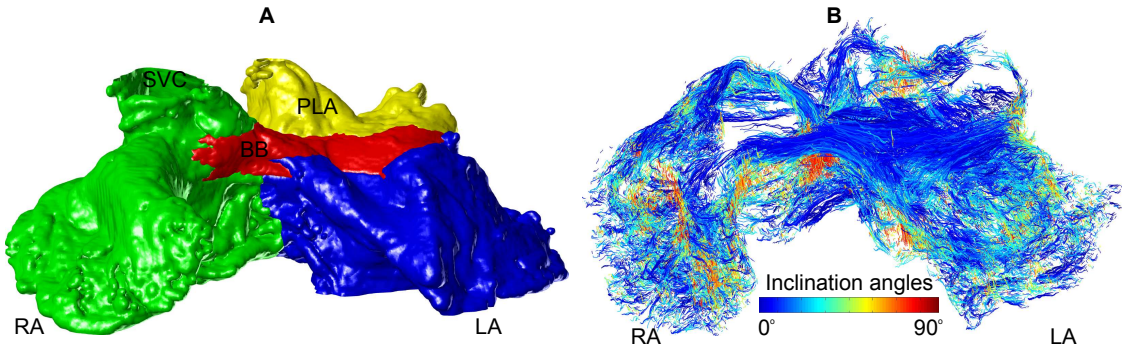

Figure 2: Anatomical structure and intramural myofiber orientation of the sheep atria. The RA and LA chambers, BB and PLA are shown in **(A)**. Atrial intramural myofiber orientation was displayed in **(B)**. Inclination angle $\alpha = 0^\circ$ is parallel to the X-Y image plane (atrio-ventricular valve plane); $\alpha = 90^\circ$ corresponds to the Z axis (inter-atrial septum)

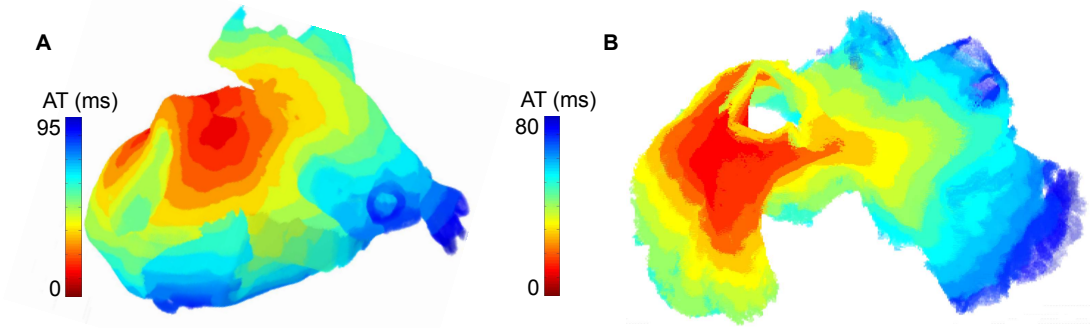

Figure 3: Activation time was superimposed on the 3D human **(A)** and sheep **(B)** atrial structure after incorporating Fenton-Karma activation models. Stimulus was delivered at sinus node for both models.

bundle structures. For major muscle bundles (e.g. CT) or circular geometry (e.g. pulmonary veins (PV)), a corridor along specific planes derived from three seed or auxiliary points was created as a boundary condition for the fast marching algorithm to ensure that the regional fiber orientation followed the expected pathway, for further detail see [5]

B. Structure-tensor based fiber generation

Methods for estimating fiber orientations have been developed extensively in materials science over the past twenty years because of the need to describe the structure of many fiber-based materials. For example, the distribution of fiber orientations in ordinary, everyday-used paper influences its physical properties such as strength, stiffness, and hygroexpansion.

In its simplest form, characterization of fiber orientation was performed by manual measurement on histologic sections. The manual estimation of angles is error-prone, subject-dependent, and time consuming. Automated methods for assessing 2D fiber orientation make use of image processing approaches, the most popular one of which uses gradients of color intensity [8]. The local orientation (x, y) of the image section I is determined by the ratio of the horizontal gradient $I_x(x,y)$ and vertical gradient $I_y(x,y)$. This is a powerful technique in 2D, however, direct extension of this method into 3D volume images does not give reliable orientation information.

The structure tensor method generalizes the gradient based approach so that it can be applied to 3D problems [9]. In order to study orientations instead of directions, structure tensor matrix J is proposed as the tensor product of the gradient vector, i.e.,

$$J = \begin{bmatrix} I_x \cdot I_x & I_x \cdot I_y & I_x \cdot I_z \\ I_y \cdot I_x & I_y \cdot I_y & I_y \cdot I_z \\ I_z \cdot I_x & I_z \cdot I_y & I_z \cdot I_z \end{bmatrix}$$

The 3×3 structure tensor J contains gradient information at each voxel in a 3D volume in the form of a matrix [10]. The tensor field is then averaged and smoothed by convolving it with a Gaussian kernel of standard deviation ρ:

$$J_\rho = J * \rho$$

By the way it is constructed, the structure tensor matrix J is symmetric and positive semi-definite, and has full ranks. As we can see, the structure tensor J is a representation of average orientation information, an inherently periodic quantity, over an entire neighborhood. This is the reason that the structure tensor has an advantage over other conventional representations, e.g. angles or vectors, and can generate more robust orientation information from the underlying 3D volume images [11]. The local orientation can be retrieved from the tensor by expanding the tensor in terms of its eigenvectors w_i and eigenvalues λ_i (i = 1, 2, or 3) in decreasing order of magnitude. The eigenvectors w_i are aligned with the intensity variations in the neighborhood. Local fiber alignment is modeled as the orientation with the least signal variation; this corresponds to the eigenvector w_3. Finally, the fiber field is further smoothed by averaging fiber orientations in the neighborhood of each voxel.

C. Analyzing tools of fiber orientations

Similarly to ventricular study, atrial myofiber orientation is specified by defining two angles [7] the inclination angle α and transverse angle β. The inclination angle α is more relevant here and defined as: the projection of the fiber vector onto a vertical plane parallel to the epicardial or endocardial surface, measured with respect to the horizontal.

To better present myofiber orientation, atrial fiber tracts are reconstructed by tracking 3D trajectories defined by myofiber orientations within regions of interest using a simple line interpolation algorithm [12]. The tract is propagated iteratively from a selected seed point, moving an incremental distance in the local myofiber direction (estimated by averaging 8 neighboring orientation vectors) with each cycle.

D. Computational models

Computational simulations were performed in one human model (MRI, with a resolution of $0.33\times0.33\times0.33$ mm^3) with rule-based atrial fiber orientation and one sheep atrial model (with a resolution of $0.2\times0.2\times0.2$ mm^3) with structure-tensor-based myo-architecture to compare the impact of the differences in description of anisotropy on atrial excitation. Cell coupling was described by the mono-domain equation in both models [4]. Electrical properties were assumed to be axially anisotropic within connected myocyte layers or bundles. Ratios for transverse to longitudinal conductivity were set to 1:10 throughout the atrial chambers. A Fenton-Karma kinetic activation model was adapted in this work [13], [14].

III. Results

A. Myofiber orientation

Anterior and posterior views of the epicardial surface of human atria are displayed in Figure 1A and 1B, respectively; while a similar anterior view of sheep atria is shown in Figure 2A. The position and shape of different atrial features (e.g., BB, superior vena cava (SVC), pulmonary veins (PV), right atrium (RA), left atrium (LA), posterior LA (PLA)) in the two models appear different partially due to the two different acquisition techniques (MRI and confocal imaging) and view orientation. However, myofiber arrangement appears consistent across the two models. Myofiber structure, visualized using fiber tracking techniques, is rendered on an anterior and posterior views of the human atria in Figure 1C and 1D and on an anterior view of the sheep atria in Figure 2B. The circumferential orientation of myofibers at the base of the SVC and around the PV are evident. Also clear is myo-structure along BB, which originates near the anterior junction of SVC and RA, and runs leftward, near parallel to the X-Y plane across the inter-atrial groove to the LA. Other features common in the two models are the uniformly longitudinal orientation of myofibers in much of the inter-atrial septum and also the septo-pulmonary bundle (SPB) between right and left PVs in the PLA wall.

B. Electrical activation

Stimulus was delivered at the location of the SAN in both models. Activation time (AT) is superimposed on the 3D human and sheep atrial structure in Figure 3A and 3B respectively. Time to full activation is $\sim$95 ms for human and $\sim$80 ms for sheep. The different position and shape of atrial tissue structures between the human and sheep models make quantitative comparison of activation pattern difficult. However, preferential propagation pathways on the epicardial surfaces are qualitatively similar. Firstly, rapid spread of activation is observed from the SAN across the superior RA into the right atrial appendage (RAA) and from the RA to LA along BB. The role of the CT and pectinate muscles (PM) in the activation of the RAA is demonstrated by the fact that epicardial activation reflects PM structure. The effects of preferential axial conduction in the atrial septum and to a lesser extent the functional extension of BB across the anterior surface of the LA are also clear. Finally, activation spreads more rapidly across the LA roof along the SPB.

IV. Discussion and Conclusions

The crucial role of atrial anatomy and myoarchitecture in AF is well recognized. It has been demonstrated that there are two different types of conduction block and reentry in the region of PM and CT deep to the atrial epicardial surface due to bundle geometry and myofiber orientations [8]. Hocini and colleagues observed activation delay in canine PV due to sudden myocardial fiber orientation changes [15]. With dramatically improved imaging techniques, e.g., confocal microscopy, researchers can acquire atrial tissue structure up to $\sim$1 μm spatial resolution [16]. However, obtaining realistic atrial myofiber orientation descriptions and incorporating them into computational models is still a major challenge. Recently, Krueger and co-workers have developed a novel semi-automatic rule-based approach to generate atrial fiber descriptions throughout the atrial walls in patient-specific geometries. Their rule-based algorithm ensures that major longitude or circular bundles are well characterized, and in regions without muscular bundles there is a smoothed description of fibre [5]. This approach is certainly efficient, however, its accuracy in some regions, for example the left atrial wall, is subject to doubt [1]. Zhao and colleagues have generated atrial myofiber orientations using the structure tensor approach [7]. The results are consistent with previous anatomic descriptions [1]. However, there is also some potentials for errors with this approach, in particular: (i) thick bands of connective tissue at the atrial surfaces and surrounding blood vessels may generate artifacts and (ii) variations in staining between serial sections gives rise to scatter and may introduce some bias.

In this study, we have compared two approaches for generating model descriptions of atrial wall fiber orientation fields. We observed similar bundle structures in the human and sheep atria, for example in BB, atrial septum, PMs, SVC and SPB. In tissue regions where major muscle bundles are absent, it is very difficult to compare the two methods because the views of the anatomical structures are quite different (Figure 1A-B and Figure 2A). However, our computational simulation confirms that the activation sequence in both atrial models is qualitatively similar and dominated by preferential propagation pathways along major muscle bundle structures.

In future, we propose to generate rule-based and structure-tensor derived atrial fiber descriptions on the same atrial geometry, and compare the two approaches by checking the 3D high-resolution tissue images obtained by the confocal imaging. By doing so, we hope to validate and improve the two fiber generation approaches and our understanding of atrial myofiber structure.

V. Acknowledgments

The authors thank three anonymous reviewers for their insightful suggestions.

References

[1] Ho SY, Sánchez-Quintana D. The importance of atrial structure and fibers. Clin Anat. 2009;22(1):52-63.

[2] Ho SY, Sánchez-Quintana D, Cabrera JA, Anderson RH. Anatomy of the left atrium: implications for radiofrequency ablation of atrial fibrillation. J Cardiovasc Electrophys. 1999;10:1522-1533.

[3] Aslanidi O, Boyett M, Li J, Dobrzynski H, Zhang H. Mechanisms of transition from normal to reentrant electrical activity in a model of rabbit atrial tissue: interaction of tissue heterogeneity and anisotropy. Biophys J. 2009;96:798-817.

[4] Seemann G, Höper C, Sachse FB, Dössel O, Holden AV, Zhang HG. Heterogeneous three-dimensional anatomical and electrophysiological model of human atria. Phil. Trans. R. Soc. A. 2006;364:1465-1481.

[5] Krueger MW, Schmidt V, Tobon C, Weber FM, Lorenz C, Keller DUJ, Barschdorf H, Burdumy M, Neher P, Plank G, Rhode K, Seemann G, Sánchez-Quintana DS, Saiz J, Razavi R, and Dössel O. Modeling atrial fiber orientation in patient-specific geometries: A semi-automatic rule-based approach. FIMH 2011, LNCS 6666, pp. 223-232, 2011.

[6] Dössel O, Krueger MW, Weber FM, Schilling C, Schulze WHW, Seemann G. A framework for personalization of computational models of the human atria. Conf Proc IEEE Eng Med Biol Soc, pp. 4324-4328, 2011.

[7] Zhao J, Butters TD, Zhang H, Pullan AJ, LeGrice IJ, Sands GB, Smaill BH. An image-based model of atrial muscular architecture: Effects of structural anisotropy on electrical activation. Circ. A&E 2012;5:361-370.

[8] Zhao J, Trew M, LeGrice I, Smaill B, Pullan A. A tissue-specific model of reentry in the right atrial appendage. J Cardiovasc Electrophys. 2009;20(6):675-684.

[9] Frangi A, Niessen W, Vincken K, Viergever M. Multiscale Vessel Enhancement Filtering. Lecture Notes in Computer Science 1998:130-137.

[10] Weickert J. Anisotropic Diffusion in Image Processing. Stuttgart, Germany: Teubner-Verlag; 1998.

[11] Ginkel MV. Image Analysis using Orientation Space based on Steerable Filters. Ph.D thesis, Delft Univ. of Tech., The Netherlands, 2002

[12] Mori S, and Zijl P. Fiber tracking: principles and strategies - a technical review. NMR in Biomedicine. 2002;15:468-480.

[13] Fenton F, Karma A. Vortex dynamics in three-dimensional continuous myocardium with fiber rotation: Filament instability and fibrillation. Chaos;1998(8):20-47.

[14] Oliver RA, Krassiwska W. Reproducing cardiac restitution properties using the Fenton-Karma membrane model. Annals of Biomedical Engineering. 2005;33:907-911.

[15] Hocini M, Ho SY, Kawara T, Linnenbank AC, Potse M, Shah D, Jaïs P, Janse MJ, Haïssaguerre M, Bakker J. Electrical conduction in canine pulmonary veins electrophysiological and anatomic correlation. Circulation. 2002;105:2442-2448.

[16] Gerneke DA, Sands GB, Ganesalingam R, Joshi P, Caldwell BJ, Smaill BH, Legrice IJ. Surface imaging microscopy using an ultramiller for large volume 3D reconstruction of wax- and resin-embedded tissues. Microscopy Research and Technique. 2007;70:886-894.